29th Congress of the International Council of the Aeronautical Sciences
St. Petersburg, Russia; September 7-12, 2014

FATIGUE DAMAGE DETECTION IN LARGE THIN WALL PLATE BASED ON ULTRASONIC GUIDED WAVE BY USING A PIEZOELECTRIC SENSOR NETWORK

Behrouz Alem *, Ali Abedian **
***Aerospace Engineering Department, Sharif University of Technology, Tehran, Iran**
mail: b_alem@ae.sharif.edu, phone+98-(0)21-661-4647

Keywords: *Structural health monitoring, piezoelectric sensor, guided waves, baseline-free damage detection*

Abstract

Today, structural Health monitoring is a major concern in the engineering community. Multisite fatigue damage, hidden cracks and corrosion in hard-to-reach locations are among the major flaws encountered in today's extensive diagnosis and/or prognosis of aircraft structures. Ultrasonic waves, lamb waves are particularly advantageous because of their propagation at large distances with little damp in thin-wall structures. In this paper a new rectangular shape array of embedded piezoelectric sensors is developed to detect some damages in large planar structures. An artificial neural network is trained to identify the damage state and its location. Output signals of each sensor due to various crack size and crack location are obtained by Finite element simulation.

1 Introduction

Many airplanes flying now have exceeded their design life and the maintenance of these aging aircraft structures has been a worldwide issue. The need for fast, low cost, and reliable monitoring system to ensure the safety and functionality of such structures is increasing and has caught the attention of many scientists in this area of research. The use of guided elastic waves, especially lamb waves, in thin plate structures has shown promises in detecting localized damages such as cracks or corrosion due to the relatively short wave length of the propagating waves. Several studies have shown that guided waves can travel large distances in thin plate structures and have good characteristics such as transmission, reflection, scattering and absorption of acoustic energy for identifying damages such as fatigue crack and corrosion in metallic and composite structures [1-10]. Giurgiutiu and Bao [11] coined the name Embedded Ultrasonic Structural Radar (EUSR). In the EUSR concept the Lamb Waves are generated over a long-range using a number of piezoelectric wafers arranged into a uniform line array and integrated with the inspected plate structure. Yu and Giurgiutiu [12], used the phased array in situ transducers to visualize the defect location and size in thin wall structures. Engholm and Stepinski [13] used uniform circular phased arrays for structural health monitoring of large planner structures. Some other researchers employed various arrangements of piezoelectric transducers and probabilistic methods for locating and characterizing cracks in a plate like structure [14-17]. However, the propagation of lamb wave is so complicated that is difficult to understand and interpret. On the other hand, conventional SHM techniques using guided waves are based on the comparison of testing data to the corresponding baseline data. Normally, baseline data are recorded when a structure is in pristine condition. The major concern is that environmental and operational effects such as changes in temperature, surface moisture, and operational loads can produce significant changes in response signals and

make it difficult to identify the structural defects [18].
Since it is extremely difficult and impractical to obtain the required initial data sets in any operational and environmental conditions, in recent years some researchers have focused on the baseline-free damage identification approaches to overcome this concern [19-26]. The concept behind of these approaches is based on that the transducers are arranged on a structure such that the captured signal from sensor-actuator paths with same features can be used as a baseline.
In this article, a rectangular array of 24 embedded piezoelectric sensors on surround of a thin wall aluminum plate and a transducer as an actuator at the middle of plate are used for monitoring and detection of size and location of a damage like crack in the structure. Finite element method is used to simulate the wave propagation in the structure and the numerical output results are utilized for signal processing. It is notable that a verified and validated numerical simulation can help to design an effective array of sensors and selection of a benefitial damage index for detection and localization of various damage scenarios without any practical cost and examination. The cross correlation analysis is utilized as a damage index for detection scheme in pith-catch mode.

2 Model description and numerical setup

Several researchers have used the finite element method to simulate the propagation of lamb wave in metal and composite plate structures [27-32].
In this study, propagation of Lamb waves in a square aluminum plate was numerically simulated using the dynamic explicit time step analysis capability of ABAQUS 6.12, an existing standard commercial Software. The model domain is 400 mm by 400 mm, 1.6 mm thick aluminum plate and contains 25 embedded rectangular transducers (7mm by 7mm, 0.254 mm thick). A rectangular array of 24 embedded piezoelectric sensors on surround of a thin wall aluminum plate and a transducer as an actuator at the middle of plate are used to identify the fatigue cracks in the structure. In this arrangement, only one transducer (middle transducer) was utilized as an actuator.
The stability and accuracy of the numerical solution depend upon the temporal and the spatial resolution of the analysis. In most studies in the literature, a minimum 20 points per cycle at the highest frequency have been determined for time step (Δt) resolution. Usually for spatial accuracy, finite element size is limited to one tenth of the wavelength of the A_0 (the antisymmetric) mode, and at least two elements through the thickness of the plate, that is;

$$\Delta t < 1/(20 f_{max}),\ L_{min} \leq \lambda/10 \qquad (1)$$

Both piezoelectric transducer and aluminum plate were simulated with 3D eight node standard element with three degrees of freedom per node in ABAQUS library. The lower surface of piezoelectric transducer was attached to the aluminum plate by 'tie' constraint in ABAQUS standard and it has been tried that the mesh pattern of the two connected regions be same. In tied surface of actuator transducer is considered as a master region, however, the sensor surface is assumed as a slave region. Modeling of piezoelectric tied to the structure causes to achieve a more realistic simulation because the elastic effects of them are considered. The following properties were assumed for the isotropic material of the aluminum plate: ρ=2700kg/m3, Young's modulus E=70.0GPa, shear modulus G=25.94GPa, and Poisson ratio ν=0.33. Also, the orthotropic properties were defined for piezoelectric transducers as followed: ρ=7700 kg/m3, Young's modulus $E_1=E_2$ =70.0GPa in plane direction & E_3=54.0GPa in normal direction, shear modulus G=23.0GPa, and Poisson's ratio ν=0.35.
The cracks in aluminum plate were simulated as artificial cut damages (through thickness cuts of 7mm long and 0.3mm wide, shown in Fig. 1) located along the different paths at 40mm distance from the actuator transducer. For finite element modeling of the cracks or cut damages the corresponding elements were removed from the mesh.

The frequency of excitation signal is the other important parameter that must be selected carefully. The frequency must be chosen such that, only the first fundamental symmetric S_0 and antisymmetric A_0 modes to get excited in the structure. The symmetric and antisymmetric modes of output signals will then be separated in pitch-catch method. This is dependent on the distance of the actuator and sensor transducers and velocity of the symmetric and antisymmetric waves or time flight of the waves.

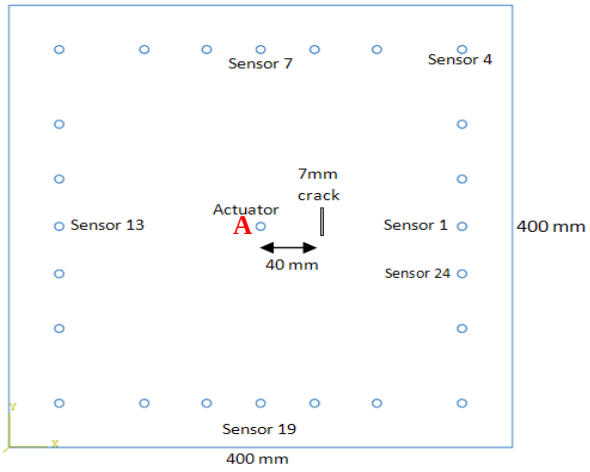

Fig.1. Location of damage and of the transducer array (dimensions are in mm)

Therefore, a four-cycle sinusoidal tone burst electrical potential function having a 300-KHz center frequency and ten volt amplitude, pick to pick, was chosen for the actuator signal. Figs 2 (a) and (b) exhibit a Hanning windowed excitation signal of 300 KHz in the time and frequency domains, respectively.

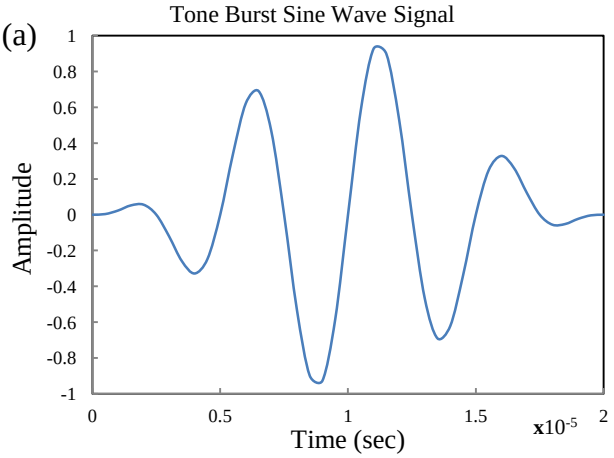

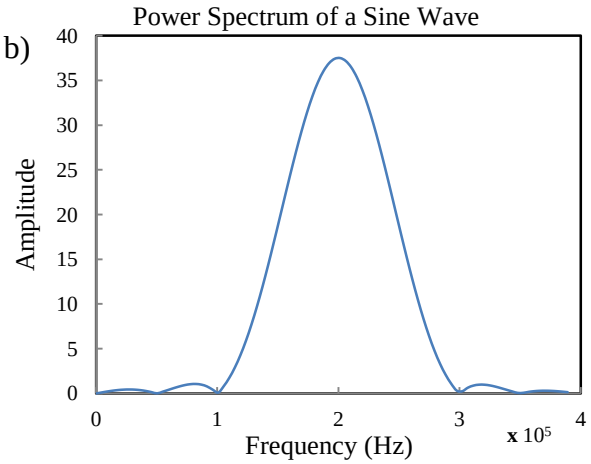

Fig. 2. a) 4-cycle tone burst, b) fast Fourier transform of the 4-cycle tone burst.

For numerical modeling, the excitation wave is actuated in the structure by applying the loads to the nodes of the transducer elements. Bagheri et al. [26] have applied the excitation wave as out of plane nodal forces to the nodes of the structure that correspond to the middle point of the lower surface of the piezoelectric actuator attached to the plate. This forcing function can effectively excite the antisymmetric mode A_0 in the structure, but it is no real. Cho and Linsden [32] applied the pin force to the nodes around the perimeter of the transducer footprint, but the bending moments due to bending strain of transducer element were neglected. In this article, the electromechanical coupling equation of piezoelectric material was used to calculate the actuator forces. The constitutive equations describing the piezoelectric actuator property are based on the assumption that the total strain in the transducer is sum of the mechanical strain induced by mechanical stress and the controllable actuation strain caused by the applied electric voltage as follows [33]:

$$E=S^E\sigma+d.E \qquad (2)$$

where σ: stress vector, ε: strain vector, E: applied electric field vector, S^E: elastic compliance matrix and d: matrix of piezoelectric strain constants. Fig. 3 illustrates the distribution of the calculated nodal forces on actuator transducer which make the equivalent excitation in the structure.

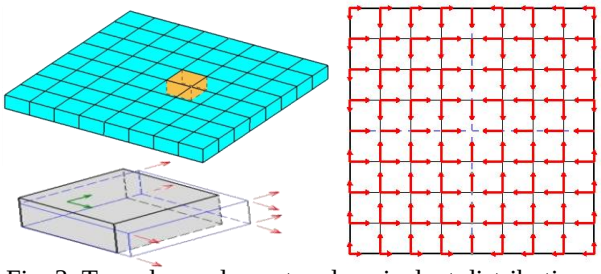

Fig. 3. Transducer element and equivalent distribution of nodal forces due to electrical strain

The finite element strain or stress results of middle element of the sensor can also be used for calculation of electric potential output of the sensor. The electromechanical equation describing the liner piezoelectric material can be written as follows [33]:

$$D=\xi^{\varepsilon} E+e.\varepsilon \quad or\ D=\xi^{\sigma} E+d.\sigma \qquad (3)$$

where D is the electrical displacement vector, e represents the piezoelectric stress constant matrix, and ξ is the permittivity.

Fig. 4 shows the contour graph of the von Misses stress at 23.5 μs, when the 4 tone burst signal was applied to the nodes of middle transducer.

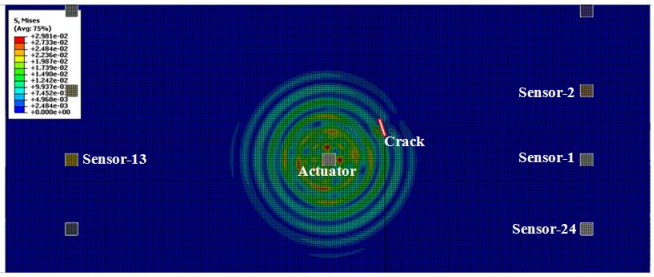

Fig. 4. von misses stress contour at time 23.5μs and when the cut damage was placed in path#3 (Units in Mpa).

3 Instantaneous Damage Identification

3.1 Detection Path of the Damage

A simple instantaneous baseline free damage detection algorithm which was proposed by Anton and Inman (2009), needs not any prerecorded data of the pristine structure. The main concept here is based on measuring the differences between the recorded signals along similar sensor-actuator paths, i. e. it relies on the fact that the recorded signals of two equal or similar paths should be identical if no defect is present in the vicinity of the paths. It is obvious that the transducers must be placed such that the paths are of equal length and that structural features are spatially uniform between transducers. When the lamb waves propagate through the structure incident to any discontinuity, transmission and reflection phenomena will be occurring and the comparison of differences in measured signals can be used to characterize the damages. In the present article, cross correlation algorithm was employed to identify the damaged path from the 24 paths shown in Fig. 1. Cross correlation analysis determines the degree of similarity of the two measured signals and can be expressed in terms of the linear correlation coefficient:

$$CC=\frac{\sum_{i=1}^{N}(x_i-\bar{x})(y_i-\bar{y})}{\left(\sqrt{\sum_{i=1}^{N}(x_i-\bar{x})^2}\right)\left(\sqrt{\sum_{i=1}^{N}(y_i-\bar{y})^2}\right)} \qquad (4)$$

where, $\bar{x}$ and $\bar{y}$ are the mean value of the two signature data sets defined as x and y. The correlation coefficient values of 1, 0, and -1 mean perfect correlation, no correlation, and perfect anticorrelation of the two signature data sets, respectively. Therefore, it is common to use "1-CC" as the damage index to have it increased by increasing the severity of damage.

$$DI\ (Damage\ Index)=1-CC \qquad (5)$$

By the arrangement of transducers illustrated in Fig. 1, the number and the location of the transducers induced a total of 24 sensing paths resulting in 6 different path lengths. Table 1 clusters all the paths according to the actuator–sensor distance. It is noted that for example path #1 presents a signal from actuator transducer to sensor transducer#1, or #7, or #13 or #19.

It is necessary to note that the cross correlation damage index is more sensitive to the delay in time of the two comparing signals than the differences in their other features. It can distinguish the damage path by the amount of changes in time delay feature of the received (transmitted) signal occurred in incident of damages.

Table 1 The number of total paths and the geometric distances between each path

Actuator-sensor distance (mm)	Signal path	Total number of paths
160	Path#1, 7, 13, 19	4
165.6	Path#2, 6, 8, 12, 14, 18, 20, 24	8
184.8	Path#3, 5, 9, 11, 15, 17, 21, 23	8
226.3	Path#4, 10, 16, 22	4

3.2 Damage Location Identification

Following the detection of damaged path, the location of the damage (distance from the actuator) is the other damage parameter that should be characterized. Measuring the flight time of the wave reflected or scattered from the discontinuity like damage is the best parameter which can be utilized to identify the damage location. In the wave propagation approach, the pulse-echo and acousto-ultrasonic methods, in which the actuating and receiving transducer are the same, can be utilized to identify the additional reflections generated by the crack damage. Thus, the scattered wave due to cut damage will be the remained found by subtracting the two output signals recorded from the damaged path (x) and its similar feature with no damage path (y).

$$SW=|x-y| \qquad (6)$$

Finally, the time of the flight of the scattered signal determines the location of the damage from actuator transducer according to the wave velocity in structure.

3 Damage Identification Results

As explained previously, the 300 KHz central frequency and 4 tone burst excitation wave was selected such that the separation between the fundamental symmetric and antisymmetric modes occurred after wave propagation through minimum sensing path distance. Fig. 5(a) shows a sample output signal obtained from sensor #1 (path#1) and its related packet waves. Fig. 5(b) compares the normalized of symmetric mode of output signals captured from the sensor of path#1 as a sample with crack and no crack along its direction. Time delay in output signals, caused by incidence of the cut damage can be used to recognize the damage path by using cross correlation damage index.

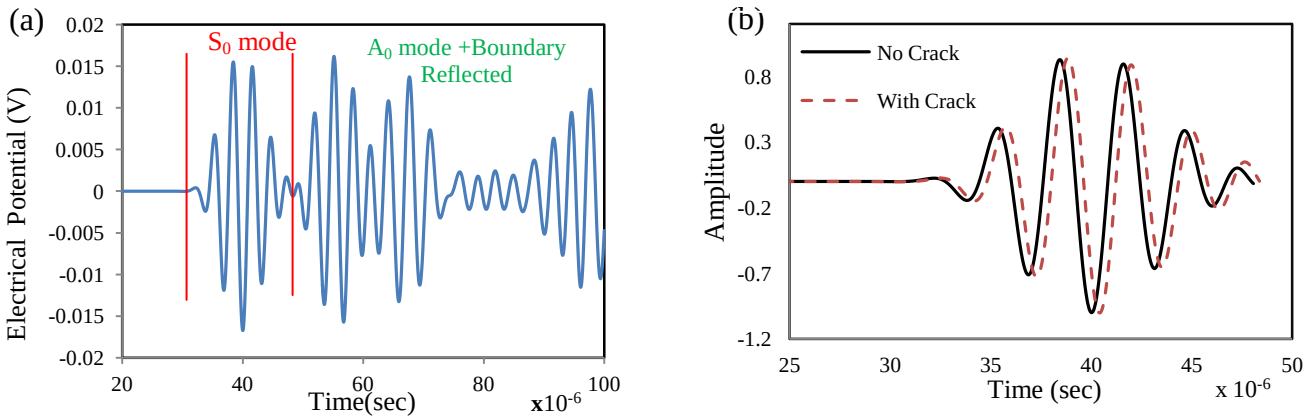

Fig. 5. a) Output signal S_0 and A_0 mode, b) Normalized captured lamb wave signals for crack and no crack path

At first, the artificial cut damage was placed along path#1 to #4 by 40mm distance from the actuator transducer because the other paths are similar to these four paths. The damage index was calculated for the twelve path combination described in table 1. Fig. 6 illustrates the damage index values related to the each damage path. The figure shows that the damage

indicators, “1-CC” values, corresponding to the damaged path combination are bigger than threshold value. The values of damage indexes are constant and near to zero with the exception of those pairs that are affected by the presence of the cut damages. As shown in Fig. 6(a) to 6(b), the damage index values of combination path 1-13, 2-14, 3-15 and 4-16 get higher value because of the damage existing in path#1, #2, #3 and #4 respectively. For example the higher value of damage index in combination path 1-13 implies the existing of the damage through the path#1 or path#13. After that, other combination index related to similar path#1 and #13 can help to recognize the damaged path from them (path 1-7, 1-19, 13-7 and 13-19).

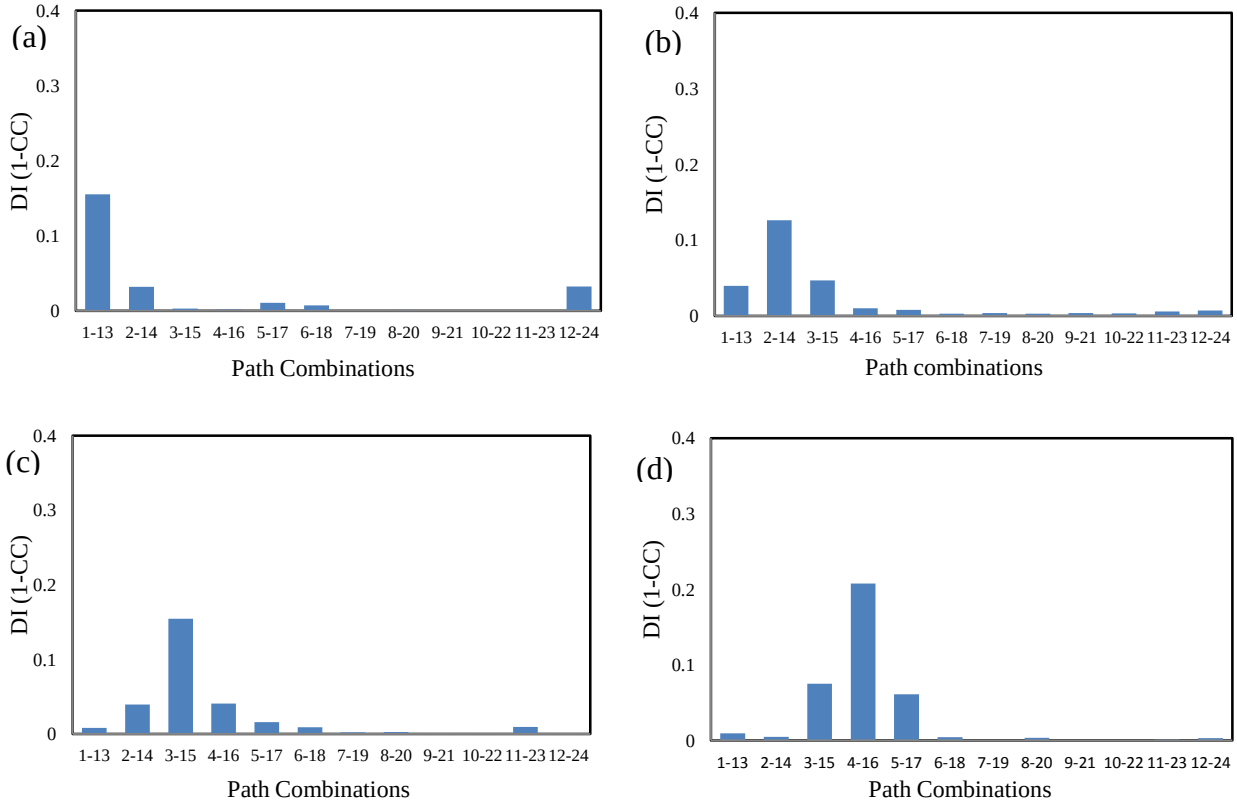

Fig. 6. Damage index values for 7 mm cut damaged existing in a) path#1, b) path#2, c) path#3 and d) path#4

As described before, the damage index values of Fig. 6(b) implies that the existing of damage through along the path#2 or path#14. It is clear that the other damage index values of those pairs combined by these two paths and their similar paths can determine the damaged path. From Fig. 7 it can be seen that the damage index values which contain the path#2 are higher than the others. It interprets the existence of damage through the path#2.

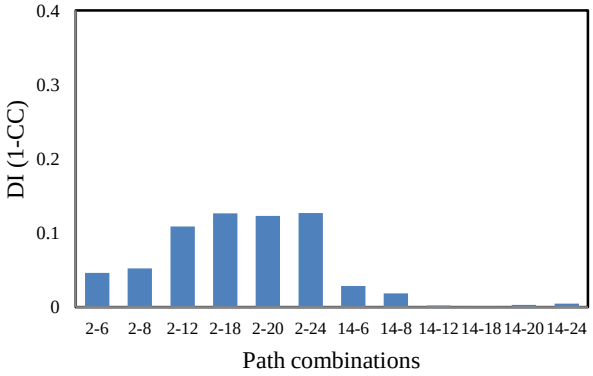

Fig. 7 Damage index values for combination of path#2 and #14

It is notable that usually in instantaneous damage detection method the existence of more than one damage path makes it difficult to determine the damaged path. This arrangement can determine the existence of multi damages until through the at least four paths. Also, it is possible to use the half symmetric of this arrangement (Fig. 1) by the one transducer actuator at the middle lower edge of plate and 13 sensors around it. The half or a quarter arrangement reduces the number of multi damages which can be detected.

In the final step, measuring the time flight of the reflected wave from the damage by using pulse-echo method has been utilized for determining the damage location. After detection of the damaged path, the excited wave will be applied through the structure by the sensor of damaged path (for example from sensor#4 in damaged path#4 Fig.1). The output signal recorded from the same transducer in pulse-echo mode. The reflected portion of the received signal due to effect of cut damage can be obtained by subtracting the output signal of the damaged path from its similar path (Path#10, or #16, or #22) regarded as the instantaneous baseline. The various cut damages are placed in along direction path#4 with various distances from middle transducer ranging from 40mm to 160 cm. Fig. 8(a) shows the scattering signals of these cases obtained by subtracting the output signal of sensor#4 in path#4 from signal of sensor#16 in path#16. The time flight of scatter wave is the time corresponding to the maximum amplitude and it is related to the reflected wave from damage. Fig. 9 (b) illustrates a good linear relationship between the flight time of scatter wave and the distance of the damage from the middle transducer along the direction of path#4.

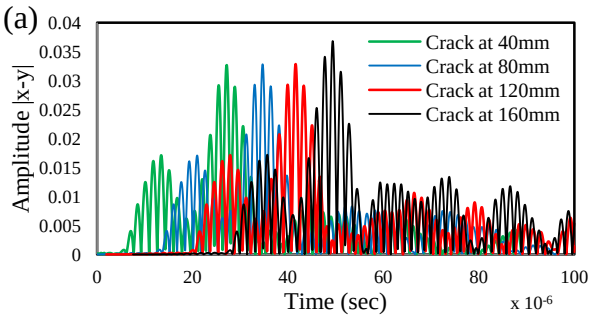

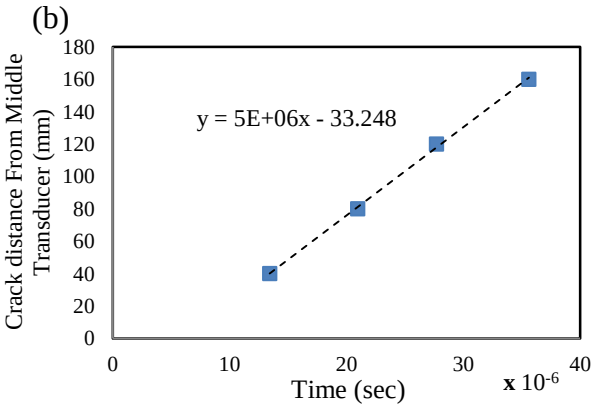

Fig. 9 (a) Reflected scattering signals caused by the cracks in different locations from the middle transducer, (b) receiving time of the reflected or scatter waveform from the cut damage to the sensor

4 Conclusions

In this study, a new sensor arrangement was proposed for damage detection based on baseline free technique, so that cracks can be detected without using any direct comparison with previously obtained baseline data. Features from the conjugate undamaged paths are used to create a statistical baseline knowledge of the structure. The proposed technique is based on the premise that the fundamental symmetric (S_0) mode attenuates when it passes through crack damage. The baseline free SHM method can be utilized for real applications under extreme environmental conditions and it will be more reliable than the conventional methods. In this arrangement, only one transducer act as an actuator in damage detection scheme. The damage index technique base on cross correlation relation and the finite element results were used to determine the location and existence of the cut damages like cracks in thin plate. Pitch-catch method was utilized to diagnosis the presence of the damage, and the Pulse-echo method was used to determine the damage location by finding the flight time of reflected scatter wave in effect of the damage. Various damage locations were examined successfully could be approximated by the proposed approach. The existence of more than one damage or multi damages is the major concern of instantaneous SHM method. The sensor arrangement

presented in this paper can be used for detection of multi damaged paths. The results of multi cracks scenarios (4 damaged paths simultaneously) can be obtained and used to train of the neural network to find the damage paths. The instantaneous damage detection approach was investigated when only the damages placed within the guided wave path. Other considerations to find the possibility of detection of damages that placed out of the guided wave paths are required in future. It is noted that the numerical simulation can reduce the cost of design SHM method containing sensor arrangements and damage index approaches for complicated structures and all multiple damage scenarios.

References

[1] Alleyne D N and Cawley P. The excitation of Lamb waves in pipes using dry-coupled piezoelectric transducers. *Journal of Nondestructive Evaluation*, Vol. 15, pp 11–20, 1996.

[2] Clarke T, Cawley P, Wilcox P D, et al. Evaluation of the damage detection capability of a sparse-array guided-wave SHM system applied to a complex structure under varying thermal conditions. *IEEE Transactions on Ultrasonics, Ferroelectrics and Frequency Control*, Vol. 56, No. 12, pp 2666–2678, 2009.

[3] Diamanti K, Hodgkinson JM and Soutis C. Detection of low-velocity impact damage in composite plates using Lamb waves. *Structural Health Monitoring*, Vol. 3, No. 1, pp 33–41, 2004.

[4] Giurgiutiu V. Tuned Lamb wave excitation and detection with piezoelectric wafer active sensors for structural health monitoring. *Journal of Intelligent Material Systems and Structures*, Vol. 16, No. 4, pp 291–305, 2005.

[5] Park HW, Sohn H, Law KH, et al.Time reversal active sensing for health monitoring of a composite plate. *Journal of Sound and Vibration*, Vol. 302, No. 1-2, pp 50-66, 2007.

[6] Raghavan A and Cesnik CES. Review of guided-wave structural health monitoring. *The Shock and Vibration Digest*, Vol. 39, No. 2, pp 91–114, 2007.

[7] Rizzo P and Lanza di Scalea F. Wavelet-based unsupervised and supervised learning algorithms for ultrasonic structural monitoring of waveguides. In: Reece PL (ed.) Progress in *Smart Materials and Structures Research*. New York: NOVA Science Publishers, pp 227–290, 2007.

[8] Su Z, Wang X, Che Z, et al. A built-in active sensor network for health monitoring of composite structures. *Smart Materials and Structures*, Vol. 15, No. 6, pp 1939–1949, 2006.

[9] Yan F, Royer RL and Rose JL. Ultrasonic guided wave imaging techniques in structural health monitoring. *Journal of Intelligent Material Systems and Structures*, Vol. 21, No. 3, pp 377–384, 2010.

[10] Zhu X, Rizzo P, Marzani A, et al. Ultrasonic guided waves for nondestructive evaluation/structural health monitoring of trusses. *Measurement Science & Technology*, Vol. 21, No. 4, pp 5701, 2010.

[11] Giurgiutiu, V and Bao J, Embedded ultrasonic Structural Radar for In-Situ Structural Health Monitoring of Thin-Wall Structures, *Structural Health Monitoring – an International Journal*, Vol. 3, No. 2, pp 121-140, 2004.

[12] Yu L and Giurgiutiu V. In situ *2-D* piezoelectric wafer active sensors arrays for guided wave damage detection. *Ultrasonics*, Vol. 48, No. 2, pp 117-34, 2008.

[13] Engholm M and Stepinski T. Direction of arrival estimation of Lamb waves using circular arrays, *Structural Health Monitoring Online*, Vol. 10, No. 5, pp 467-480, 2010.

[14] Tua P S, Quek S T and Wang Q. Detection of Cracks in Plates Using Piezo-actuated Lamb Waves. *Smart Materials and Structures*, Vol. 13, No. 4, pp 643-660, 2004.

[15] Staszewski W J, Lee B C and Traynor R. Fatigue Crack Detection in Metallic Structures with Lamb Waves and 3D Laser Vibrometry. *Measurement Science and Technology*, Vol. 18, No. 3, pp 727-739, 2007.

[16] Ihn J B. Pitch-Catch active sensing methods in structural health monitoring for aircraft structures. *Structural Health Monitoring*, Vol. 7, No.1, pp 5-19, 2008.

[17] Dehghan Niri E and Salamone S. A probabilistic frame work for acoustic emission source localization in plate-like structures. *Smart Materials and Structures*, Vol. 21, No. 3, pp 5009, 2012.

[18] Sohn H. Effects of environmental and operational variability on structural health monitoring. *Phil. Trans. R. Soc. A.*, Vol. 365, No. 1851, pp 539-560, 2007.

[19] Sohn H, Park HW, Law KH, et al. Combination of a time reversal process and a consecutive outlier analysis for baseline-free damage diagnosis. *Journal of Intelligent Material Systems and Structures*, Vol. 18, No. 4, pp 335–346, 2007.

[20] Anton SR, Inman DJ and Park G. Reference-free damage detection using instantaneous baseline measurements. *AIAA Journal*, Vol.47, No. 8, pp 1952–1964, 2009.

[21] Kim MK, Kim EJ, An YK, et al. Reference-free impedance-based crack detection in plates. *Journal of Sound and Vibration*, Vol. 330, No. 24, pp 5949–5962, 2011.

[22] Lee SJ, Gandhi N, Hall JS, et al. Baseline-free guided wave imaging via adaptive source removal. *Structural Health Monitoring*, Vol. 11, No. 4, pp 472-481, 2012.

[23] Park S, Lee C-G and Sohn H. Reference-free crack detection using transfer impedances. *Journal of Sound and Vibration*, Vol. 329, No. 12, pp 2337-2348, 2009.
[24] Park S, Anton S-R, Kim J-K, Inman D-J and Ha D-S. Instantaneous baseline structural damage detection using a miniaturized piezoelectric guided waves system. *KSCE Journal of Civil engineering*, Vol. 14, No. 6, pp 889-895, 2010.
[25] Qiang W and Shenfang Y. Baseline-free imaging method based on new PZT sensor arrangements. *Journal of Intelligent Material Systems and Structures*, Vol. 20, No. 14, pp 1663–1673, 2009.
[26] Bagheri A, Li K and Rizzo P. Reference-free damage detection by means of wavelet transform and empirical mode decomposition applied to Lamb waves. *Journal of Intelligent Material Systems and Structures*, Vol. 24, No. 2, pp 194–208, 2012.
[27] Alleyne DN and Cawley P. A two dimensional Fourier transform method for measurement of propagating multimode signals. *Journal of the Acoustical Society of America*, Vol. 89, No. 3, pp 1159–1168, 1991.
[28] Bartoli I, Lanza di Scalea F, Fateh M, et al. Modeling guided wave propagation with application to the longrange defect detection in railroad tracks. *NDT & E International*, Vol. 38, No. 5, pp 325–334, 2005.
[29] De Marchi L, Marzani A, Speciale N, et al. Prediction of pulse dispersion in tapered waveguides. *NDT & E International*, Vol. 43, No. 3, pp 265–271, 2010.
[30] Moser F, Jacobs LJ and Qu J. Modeling elastic wave propagation in waveguides with the finite element method. *NDT & E International*, Vol. 32, No. 4, pp 225–234,1999.
[31] Sale M, Rizzo P and Marzani A. Semi-analytical formulation for the guided waves-based reconstruction of elastic moduli. *Mechanical System and Signal Processing*, Vol. 25, No. 6, pp 2241–2256, 2011.
[32] Cho H. and Lissenden C J. Structural health monitoring of fatigue crack growth in plate structures with ultrasonic guided waves. *Structural Health Monitoring*, Vol. 11, No. 4, pp 393-404, 2012.
[33] Institute of Electrical and Electronics Engineers Inc. IEEE standard on piezoelectricity. ANSI/IEEE Std. 176–1987, 1988.

Copyright Statement